Surface Acoustic Wave Measurements Using an Impulsive Converging Beam

doi: 10.1063/1.332667

Surface acoustic wave measurements using an impulsive converging beam

Kazushi Yamanaka
Mechanical Engineering Laboratory, Namiki 1-2, Sakura-mura, Niihari-gun Ibaraki 305, Japan

(Received 12 January 1983; accepted for publication 5 April 1983)

A method for velocity and attenuation measurement of leaky surface acoustic wave on small areas of a solid surface was developed. This technique uses an impulsive converging beam generated with an acoustic lens. Reflected waves from a sample consisted of the axial wave and the leaky surface wave separated in time domain. From the time interval between these waves, the velocity of the leaky surface wave is determined using an expression derived along with ray optics. Because time interval measurements do not require any mechanical scanning, they can be done without special attention paid for mechanical precision of the scanning system, enabling rapid and simple measurement. Since the impulsive wave has a broad frequency spectrum, spectroscopic analysis of leaky surface wave is also possible. Frequency dependent attenuation measurement of leaky surface acoustic waves on heat treated steels and velocity dispersion measurement of leaky surface wave on titanium nitride film on tool steel are demonstrated.

PACS numbers: 43.35.Pt

I. INTRODUCTION

In acoustic microscopy developed by Quate *et al.*[1], techniques for velocity[2] and attenuation[3,4] measurement of leaky surface waves have been developed. They utilize the phenomenon that the amplitude of the reflected wave V exhibit periodical maxima and minima as the distance z between the sample surface and the focal point of the lens varies. This periodic variation has been ascribed to the interference between the axial wave and the leaky surface acoustic wave. From the spacing between neighboring minima, the velocity of leaky surface wave is calculated, and from the depth of minima, the attenuation of the leaky surface wave is estimated. These techniques are extremely useful in the characterization of materials.

But because the scanning of an acoustic lens or sample requires special care for the mechanical precision of the driving system, it is difficult to apply this technique where rapidity and easy manipulation are required such as in in-process measurement of materials under machining, grinding, and surface treatments or two dimensional mapping of velocity and attenuation. To eliminate this restriction, Liang *et al.*[5,6] developed a new technique for velocity perturbation measurement of leaky surface wave of small areas without any mechanical scanning of the lens nor of the sample. It uses shorter tone bursts than usually used in acoustic microscopy and temporally separates the axial wave and the leaky surface wave. Their method has a potential sensitivity of one part in 10^5 change in velocity, and this is a remarkable progress because, in the $V(z)$ curve method, the sensitivity was in the order of one part of 10^3 at best. Nevertheless, there still remain some aspects to be discussed in the velocity measurement without z scanning.

First, although Liang *et al.* stated that $V(z)$ curve measurement is necessary for absolute velocity measurement, we have shown that not only the velocity perturbation but also the absolute velocity can be measured without z scanning.[7] Moreover, because they used narrow band tone bursts containing more than ten cycles of waves, the time separation of the axial and leaky surface wave might become insufficient for high velocity materials such as sapphire or silicon nitride even at large values of z. So, we discuss here the absolute velocity measurement of leaky surface wave using a broadband impulsive converging beam, including application to high velocity materials. We also mention other potential applications of a broadband pulse in velocity dispersion measurement and frequency dependent attenuation measurement of leaky surface wave.

II. PRINCIPLE OF MEASUREMENT

The reflected waves from a sample surface illuminated by a highly converging beam have many ray components, but according to Parmon and Bertoni,[8] only two components can reach the piezoelectric transducer in such a way that they can significantly contribute to the output signal. They are the leaky surface wave and the axial wave shown in Fig. 1. The axial component of the incident converging beam leaving the acoustic lens is reflected specularly at the sample surface and travels along the path $EO'E$. The leaky surface wave is excited by an obliquely incident component on the sample at Rayleigh critical angle θ_R, propagates a certain distance along the surface, and is radiated towards the lens. It is shown by the path $ABO'CD$. The traveling times of these two waves are the same when the focus O is just on the sample surface. But, when the lens is moved towards the sample, the traveling time is different.

The time interval Δt_R between the arrival of the two components at the transducer is derived from the ray model shown in Fig. 1 as

$$\Delta t_R = 2(z \tan \theta_R / v_R - z/v_R \cos \theta_R) - (-2z/v_0), \quad (1)$$

where v_0 and v_R are velocity of longitudinal wave in the coupler and leaky surface wave on the sample. The first term in the right hand is the propagation time of the leaky surface wave along the sample surface. The second term represents the decrease in the propagation time of the leaky surface wave in the coupler due to the decrease in the distance between the lens and the sample. The third term represents

 0021-8979/83/084323-07$02.40

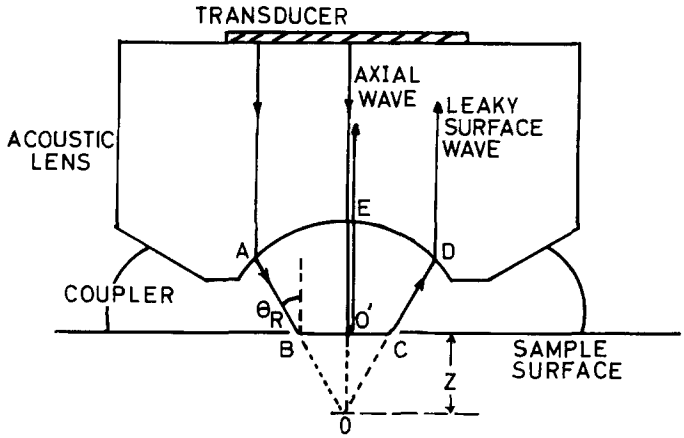

FIG. 1. Ray representation of the acoustic fields of converging beam and reflected waves. The leaky surface wave is excited by the incident ray at the Rayleigh critical angle θ_R.

the decrease in the propagation time of the axial wave. Equation (1) is reduced to a simpler form as

$$\Delta t_R = 2z(1 - \cos\theta_R)/v_0, \tag{2}$$

by eliminating v_R with the relation

$$v_R = v_0/\sin\theta_R. \tag{3}$$

From Eqs. (2) and (3) we obtain

$$v_R = (\Delta t_R/v_0 z - \Delta t_R^2/4z^2)^{-1/2}. \tag{4}$$

This is the expression to calculate v_R from the measured value of the time interval Δt_R. To measure the time interval, it is necessary to separate the axial wave and the leaky surface wave in the time domain. We realized the separation by using an impulsive converging beam.

Distance z between the sample surface and the lens focus may be set to a certain value before the measurement of the time interval, but if the surface is not flat, z may vary from point to point. Therefore it is desirable to measure z experimentally for each point of measurement. This can be done by measuring the time interval Δt_0 between the axial wave and the lens wave internally reflected at the lens–coupler interface. The time interval is equivalent to the traveling time of the longitudinal wave in the coupler along the path EO'E in Fig. 1, whose length is $2(f - z)$. Thus, we obtain the relation:

$$z = f - v_0\Delta t_0/2. \tag{5}$$

Equation (5) is used to calculate z from the known values of f, v_0 and the measured value of Δt_0. Substituting z into Eq. (4), we can calculate the velocity of leaky surface wave v_R using the measured value of Δt_R.

III. EXPERIMENTAL PROCEDURE

A. Transducer and acoustic lens

A broadband piezoelectric transducer used in this study was an air-backed 30-μ-thick PVDF film (Kureha Chemical Industry Co., Ltd.) bonded to a flat end of an acoustic lens made of fused quartz. The focal length of the lens in water used as a coupler was 4.0 mm. The lens radius was 2.7 mm, semiangle of convergence was 60°, and the length of the lens rod was 20 mm. The diameter of the rod was taken as large as 25 mm in order to supress the effect of multiple internal reflections. The antireflection coating for the lens, usually used for sapphire lenses, was not employed in order to maintain the large bandwidth.

B. Experimental apparatus

The block diagram of the measurement apparatus is shown in Fig. 2. The transducer was driven by a 30-ns, 200 V rf pulse to generate a parallel beam in the lens rod, which was transformed by the lens to a converging beam. The origin of the z axis of the sample surface was determined by adjusting a z axis stage and a two-axis tilt stage so that the amplitude of the reflected waves takes its maximum. The positive direction was defined such that the lens moves towards the sample surface. The reflected waves were detected by the same transducer, amplified by a broadband rf amplifier with 40 dB gain and recorded by a sampling oscilloscope with 1024 points digital storage with 10 bits resolution. The magnitude of the reflected waves was on the order of 100 mV after being amplified by 40 dB and the noise level was 5 mV. Consequently, the insertion loss was estimated to be 100 dB and the S/N ratio was 30 dB. The reflected waves were digitally averaged 10 times to increase the S/N ratio.

C. Background subtraction

At certain values of z, the apparent signal of reflected waves still contained a background of lens waves multiply reflected inside the lens rod due to the acoustic impedance mismatch between the lens and the surrounding media. In this case, a background subtraction procedure was performed as follows.

First, the trigger delay of oscilloscope was adjusted so that the reflected waves from a sample was properly observed in the oscilloscope and the waveform was recorded. Next, the background was recorded when sample was removed whereas the lens was still in contact with the coupler. Then the background was digitally subtracted from the apparent signal to get a true signal. An example of this procedure for SKD 11 die steel is shown in Fig. 3. In this figure, (a), (b), and (c) represent the apparent signal, the background, and the true signal after the background subtraction, respectively. The arrow in Fig. 3(a) and 3(b) indicates a contribution of the lens wave. It is obvious that the digital subtraction

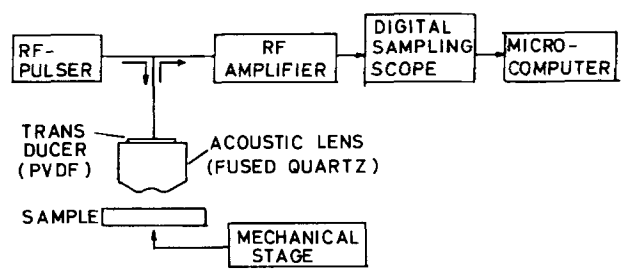

FIG. 2. Block diagram of the experimental apparatus.

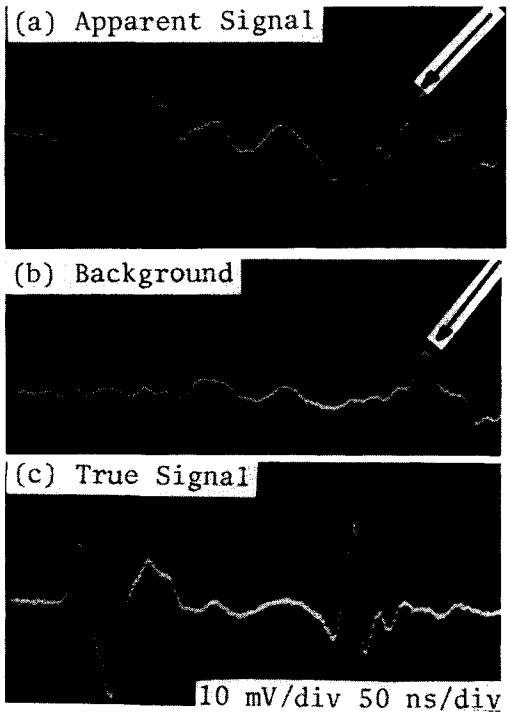

FIG. 3. Background subtraction procedure. (a) Apparent signal; (b) background; (c) true signal.

of the background served well to distinguish the true signal from the background. The resultant signal was transferred to a microcomputer where time interval measurements were performed.

D. Observation of axial wave and leaky surface wave

To get a comprehensive understanding of the critical angle phenomenon, the separation of the axial wave and leaky surface wave on soda lime glass was observed at its various stages. The reflected waves at z position of 0 to 1.0 mm are shown in Fig. 4. When the amplitude of the reflected wave was at its maximum, z was defined as 0 mm. The polarity of the pulse was negative, as was the case for the driving pulse and the lens wave reflected at the lens/coupler interface. At $z = 0.2$ mm, the amplitude of the negative peak decreased, though the leaky surface wave was not yet clearly separated. When z was increased to 0.4 mm, a positive subpulse began to separate from the main pulse. The time interval between the main pulse and the subpulse increased with increasing z. This fact suggests that the main pulse is the axial wave and the subpulse is the leaky surface wave.

The reflected waves of SKD 11 die steel, soda lime glass, Si(111) surface, and z-cut sapphire at $z = 1.5$ mm are shown in Fig. 5. Except that the magnitude of the axial waves slightly varied among the materials, their shape and width did not significantly vary. On the other hand, the interval between the leaky surface wave and the axial wave significantly decreased with increasing velocity of leaky surface wave. This result is consistent with Eq. (4).

For quantiative analyses, the time interval $\Delta t'_R$ between the negative peak of the axial wave and the positive peak of the leaky surface wave was measured. A correction

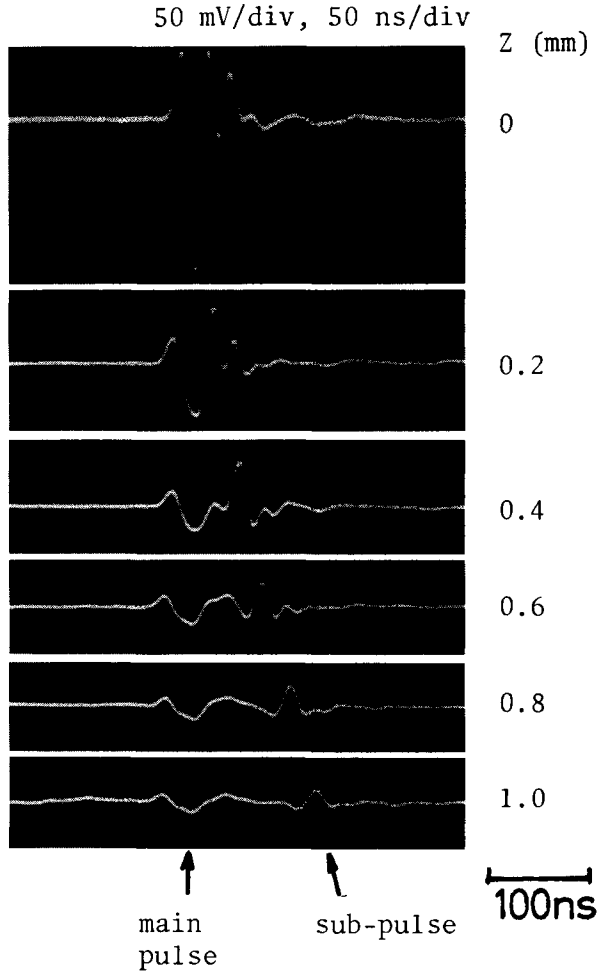

FIG. 4. Reflected waves from soda lime glass at $z = 0$ to 1.0 mm. The main pulse corresponds the axial wave and the subpulse corresponds the leaky surface wave.

factor t_c was then added to $\Delta t'_R$ to obtain the time interval Δt_R used in the comparison with the calculated values from Eq. (4). It is because the negative peak of the axial wave is slightly shifted towards the leaky surface wave by the superposition of neighboring rays whose path length is longer than that of true axial wave ($EO'E$ in Fig. 1). In Fig. 6(a) the measured time interval Δt_R at $z = 1.0$ and 1.5 mm is plotted against the velocity v_R of the leaky surface wave of each sample. The velocity of z cut sapphire and Si(111) were the velocity of Rayleigh wave on free surface averaged for [100] and [112] directions.[9] The velocity of soda lime glass and SKD 11 die steel was determined from $V(z)$ curve measurements with a 200-MHz scanning acoustic microscope. The solid curves in the figure represent the calculated values from Eq. (4). The correction factor t_c was adjusted to 24 ns so that the measured time interval Δt_R of fused quartz agrees with the calculated value. The agreement between the measured and calculated values for other materials was fairly good as shown in Fig. 6(a).

The dependence of time interval Δt_R against the distance z between the sample surface and the focus of the lens is plotted by the open circles in Fig. 6(b). The solid lines were calculated from Eq. (2). The agreement between the measured and calculated values is still good when Δt_R is more

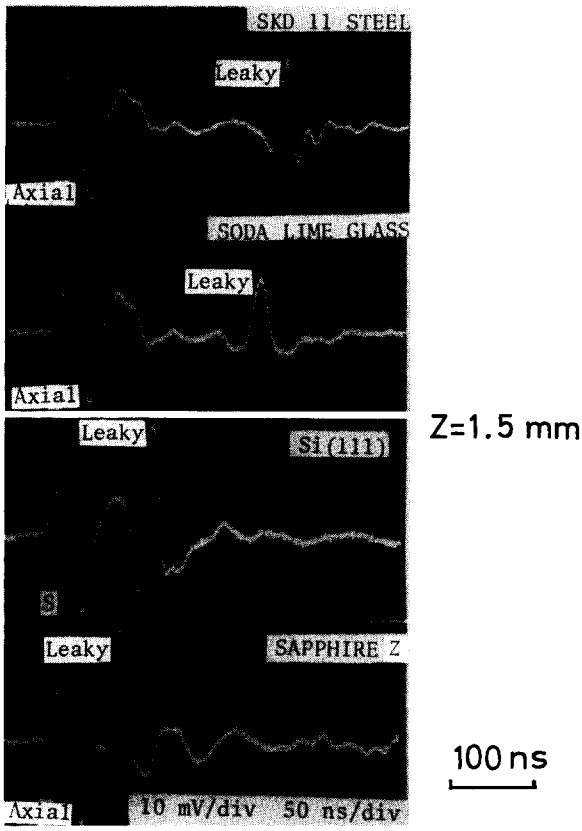

FIG. 5. Reflected waves from several materials at $z = 1.5$ mm.

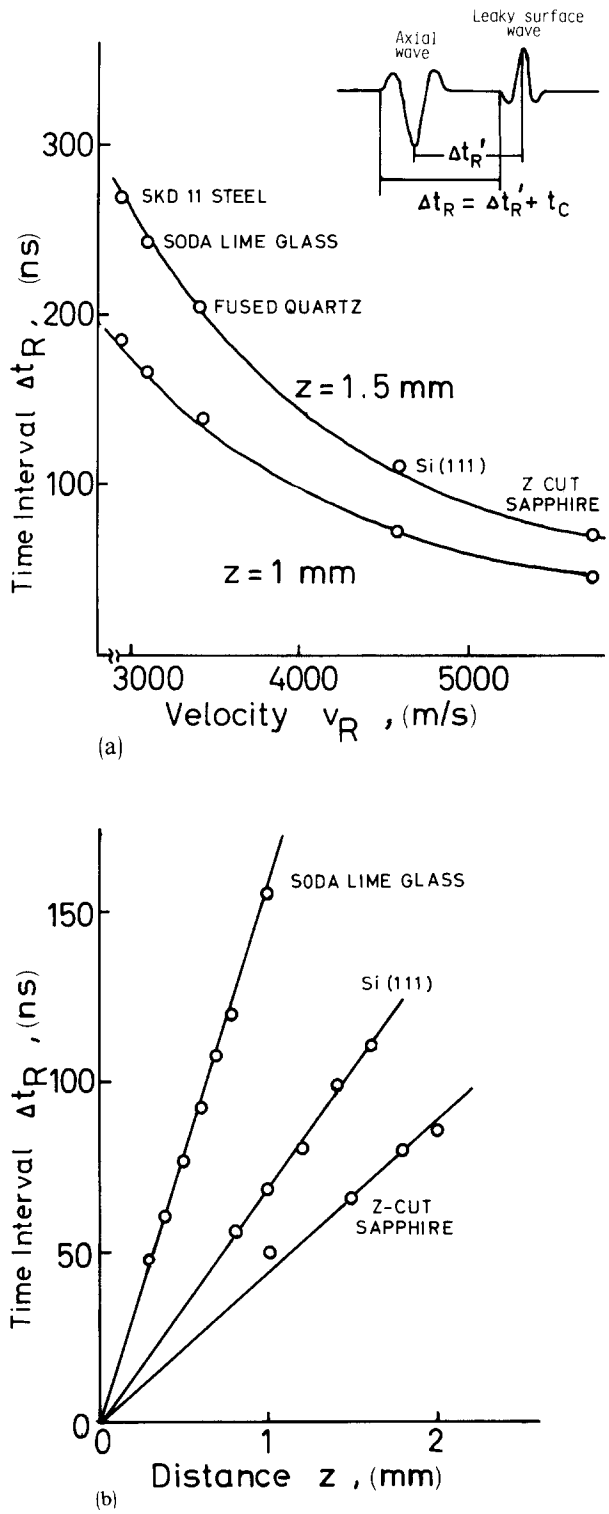

FIG. 6. (a) Dependence of the time interval Δt_R between the axial wave and the leaky surface wave upon the velocity of the leaky surface wave v_R. (b) Dependence of the time interval Δt_R on the distance z between the lens focus and the sample surface.

than 50 ns where the separation between the axial wave and the leaky surface wave is large. These results demonstrate the validity of the present method to determine the velocity v_R of leaky surface wave using Eq. (4).

IV. DISCUSSION

A. Accuracy and sensitivity

A possible difficulty in the present method may be the necessity of the correction factor t_c. But, because t_c is determined using a standard material such as fused quartz and can be fixed for all other materials, it is not a serious problem in practical applications.

To evaluate the accuracy of the present method, we compared the measured value of v_R of several materials with the calculated values, averaged for each direction in anisotropic materials. The results are shown in Table I. As seen from the table, the error was less than 3% for all materials. In anisotropic materials, the difference in the velocity of leaky surface wave v_R for each direction leads to phase differences among the received waves, which distort the waveform. This is considered to be the source of error in time interval measurement of $\Delta t_R'$. For anisotropic materials, the line focus beam developed by Kushibiki *et al.*[10] should be employed.

The sensitivity to a small change in v_R is estimated using Eq. (4). If we assume that a change in Δt_R of 1 ns is detectable at $z = 1.5$ mm, which was actually achieved in our measurement, it corresponds a change in v_R of 5.0 m/s on SKD 11 steel (0.17% of v_R) and a change of 16 m/s on z-cut sapphire (0.28% of v_R). This sensitivity is high enough to detect a small variation of heat treatment condition that affects the strength of steel or a slight change in porosity or grinding damage on sintered ceramics. It should be noted

TABLE I. Velocity of leaky surface waves. Comparison between the velocity of leaky surface wave measured by the present method and calculated values taken from the literature. For soda lime glass and SKD 11 steel, calculated values were determined from the $V(z)$ curve measurement.[2,8]

Materials	Measured v_R (m/s)	Calculated v_R (m/s)
fused quartz	...	3412
Si(111)	4558	4645
z-cut sapphire	5685	5630
soda lime glass	3142	3145
SKD 11 steel	3000	2950

that the sensitivity is higher on low velocity materials than on high velocity materials.

The major problem in our measurement is the low S/N ratio due to the low efficiency of the lens transducer system. As a result, it is necessary for realizing above mentioned sensitivity to average the signal more than ten times, reducing the rapidity of the measurement. Therefore, it is necessary to enhance the efficiency of the transducer without much reducing the bandwidth.

B. Spatial resolution

The spatial resolution of this method is determined by the extent of defocusing. Taking the radius r of the incident beam at the sample surface as a measure of the resolution, it is expressed as

$$r = z \tan \theta_R . \tag{6}$$

From the velocity data in Table I, r is estimated to be 0.41 mm for sapphire and 0.88 mm for SKD 11 die steel when z is 1.5 mm. Though the resolution is higher in sapphire than in the steel for the same value of z, z can be decreased to 0.7 mm for steel without losing the separation of the axial wave and the leaky surface wave, and hence, a resolution as high as 0.4 mm can also be obtained for steel. It is necessary to choose appropriate value of z for each material to maximize the spatial resolution.

C. Velocity dispersion measurement

Since the broadband beam is a superposition of acoustic waves with different frequencies, care should be taken when the leaky surface wave is dispersive, that is, the velocity v_R varies as a function of the frequency f. Because the phase of each frequency component of the leaky surface wave differs after propagating along the surface, the waveform of the leaky surface wave will be different from that of dispersionless case. In this case, the straightforward method of time interval measurement stated in Sec. III. D cannot be applied. But, in this case, we can measure the frequency dependent velocity of leaky surface wave with a spectroscopic analysis similar to that described by Sachse and Pao.[11]

Frequency dependent velocity $v_R(f)$ of the deposited sample is calculated as a direct extension of Eq. (4) as

$$v_R(f) = [\Delta t_R(f)/v_0 z - \Delta t_R(f)^2/4z]^{-1/2}, \tag{7}$$

where $\Delta t_R(f)$ is a frequency dependent time interval between the axial wave and the leaky surface wave. If we know the velocity of leaky surface wave on the substrate $\Delta t_R(f)$ is expressed as

$$\Delta t_R(f) = \Delta t_R^s - [\phi(f) - \phi^s(f)]/2\pi f, \tag{8}$$

where Δt_R^s is frequency independent time interval on the substrate, and $\phi(f)$ and $\phi^s(f)$ are the phase spectra of the leaky surface wave on the deposited sample and on the substrate. Δt_R^s can be measured as described in Sec. III if the substrate is dispersionless. Substituting Eq. (8) into Eq. (7), the frequency dependent velocity $v_R(f)$ is calculated.

As a typical case, we examined a systematic variation of leaky surface wave velocity due to the deposition of titanium nitride thin film[12] on a martensitic die steel (SKD 11) substrate. The reflected waves from the samples were recorded at $z = 1.5$ mm. The leaky surface wave windowed from the reflected waves for film thickness h of 0, 1.4, 4.3, and 8.6 μm, are shown in Fig. 7(a). The 20-dB bandwidth of the leaky surface wave on the substrate was 50 MHz. As the film thickness h increased, the leaky surface wave shifted towards the left, the amplitude of negative going pulse increased, and the duration increased. This behavior will certainly be ascribed to superposition of multiple frequency components of the leaky surface wave with different velocity due to the existence of velocity dispersion.

Phase spectra were obtained from Fourier transform of windowed leaky surface waves in Fig. 7(a), and the frequency dependent velocity was calculated with Eq. (7) and plotted in Fig. 7(b). As seen from the figure, v_R increased as the frequency f increased. It is because the velocity of leaky surface wave on titanium nitride is higher than that on SKD 11 steel and larger part of the energy of leaky surface wave is concentrated within a film as the frequency increases. Open circles represents measured velocity of leaky surface wave on each sample with the $V(z)$ curve measurement at 50 MHz. These were approximately equal to those determined with the present analysis. The small discrepancy may be due to ripples in phase spectra caused by the windowing.

D. Frequency dependent attenuation measurement

Besides the velocity dispersion measurement, frequency dependent attenuation of leaky surface wave can be estimated from the amplitude spectra of the leaky surface wave. As an example, the leaky surface wave on S45C steel (0.45% carbon) was examined. The surface layer as thin as a few hundred microns was locally hardened to increase wear resistance using the transformation hardening technique by electron beam.[13]

The leaky surface waves windowed from the reflected waves at $z = 1.5$ mm of three different areas are shown in Fig. 8(a). Area A is the hardened area, C is the unhardened area, and B is the boundary between the hardened and unhardened areas, where the thickness of the hardened layer is 50 to 100 μm. The amplitude of the leaky surface wave decreased and the width increased in the order of A, B, and C. The frequency spectra of these leaky surface waves are shown in Fig. 8(b). The high frequency components of the leaky surface wave in areas B and C were smaller than that in area A, indicating frequency dependent attenuation in B and

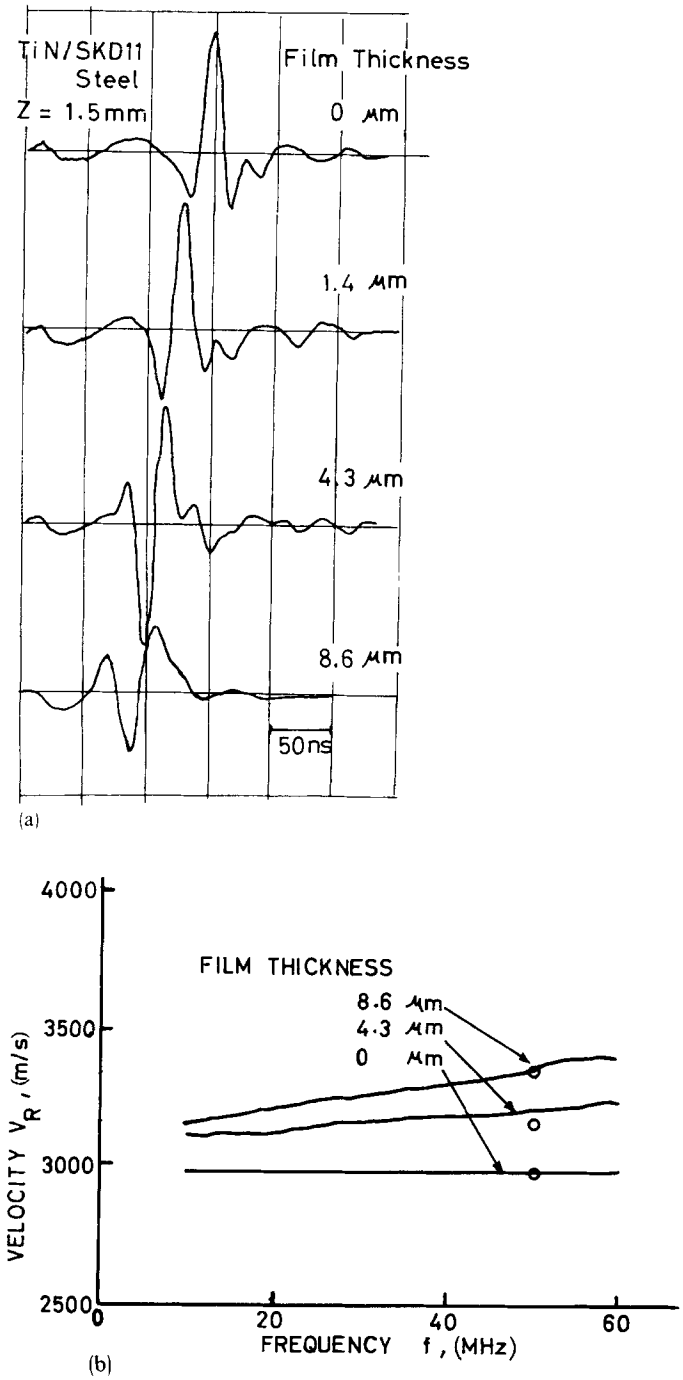

FIG. 7. Velocity dispersion on SKD 11 steel upon which titanium nitride thin film is deposited. (a) Leaky surface wave from the deposited sample at $z = 1.5$ mm. Film thickness varied from 0 to 8.6 μm. (b) Velocity of leaky surface wave as a function of frequency. Open circles represent measured values with the $V(z)$ curve measurement.[2,8]

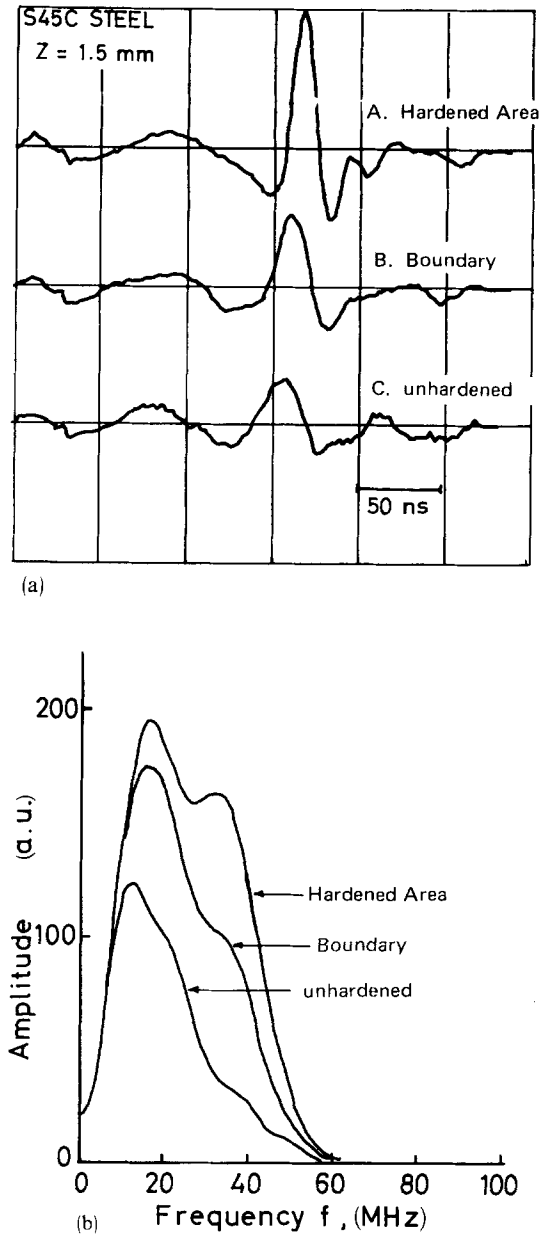

FIG. 8. Frequency dependent attenuation of leaky surface wave on transformation hardened steel by electron beam. (a) Leaky surface wave from three different areas. A is hardened area, C is unhardened area, and B is the boundary. (b) Frequency spectra of the leaky surface waves indicating frequency dependent attenuation.

C as compared with A. This attenuation is due to the larger grain size ferrite plus pearlite phase in the unhardened area than that of martensitic phase in the hardened area.[4,14] So, this measurement is useful for nondestructive testing of steels whose surface layer is locally transformation hardened.

V. CONCLUSION

Using an impulsive converging beam, we have developed a technique to measure the absolute velocity, frequency dependent velocity, and attenuation of leaky surface wave on small areas of solid surfaces without any mechanical scanning. Combining these features, it will be possible to develop a new quantiative acoustic microscope in which each parameter is mapped independently. In usual acoustic microscopy, the contrast reversal phenomenon due to the z variation is observed as a result of the interference between the axial wave and the leaky surface wave. It causes a certain complication in interpreting the acoustic image, though favorable for detecting a small change in overall acoustic properties of the sample. A new acoustic microscope proposed above is free from such a complication. Though the attempt described in this report is preliminary, and much work is need-

ed concerning instrumentation and analysis, it will provide a useful method in acoustic microscopy both for imaging and measurement.

ACKNOWLEDGMENTS

The author would like to thank Mr. A. Iwata, Mechanical Engineering Laboratory, for providing a transformation hardened S45C steel sample. He also thanks staffs in Kureha Chemical Industry Co., Ltd. for providing PVDF films.

[1]C. F. Quate, A. Atalar, and H. K. Wickramasinghe, Proc. IEEE **67**, 1092 (1979).
[2]R. D. Weglein, Appl. Phys. Lett. **34**, 179 (1979).
[3]R. D. Weglein, Electron. Lett. **18**, 20 (1982).
[4]K. Yamanaka, Electron. Lett. **18**, 587 (1982).
[5]K. Liang, S. D. Benett, B. T. Khuri-Yakub, and G. S. Kino, 1982 IEEE Ultrasonics Symposium Proceedings (604).
[6]K. Liang, S. D. Benett, B. T. Khuri-Yakub, and G. S. Kino, Appl. Phys. Lett. **41**, 1124 (1982).
[7]K. Yamanaka, 1982 IEEE Ultrasonics Symposium Proceedings (609).
[8]W. Parmon and H. L. Bertoni, Electron. Lett. **17**, 520 (1981).
[9]A. J. Slobodnik, E. D. Conway, and R. T. Delmonico, Microwave Acoustic Handbook Vol. 1A Surface Wave Velocities (AFCRL-TR-73-0597, Air Force Cambridge Research Laboratories, Massachusetts, 1973).
[10]J. Kushibiki, A. Ohkubo, and N. Chubachi, Electron. Lett. **17**, 534 (1981).
[11]W. Sachse and Y. H. Pao, J. Appl. Phys. **49**, 4320 (1978).
[12]Y. Enomoto, K. Yamanaka, and K. Mizuhara, International Conference on Vacuum Metallurgy Proceedings (The Iron and Steel Institution of Japan, 1982), p. 209.
[13]A. Iwata, J. Jpn. Soc. Precis. Eng. **48**, 91 (1982).
[14]E. P. Papadakis, J. Appl. Phys. **35**, 1474 (1964).